Free Radical Biology & Medicine, Vol. 34, No. 4, pp. 465–477, 2003

0891-5849/03/$–see front matter

doi:10.1016/S0891-5849(02)01325-4

*Original Contribution*

# DPI INDUCES MITOCHONDRIAL SUPEROXIDE-MEDIATED APOPTOSIS

NIANYU LI,* KATHY RAGHEB,* GRETCHEN LAWLER,* JENNIE STURGIS,* BARTEK RAJWA,* J. ANDRES MELENDEZ,† and J. PAUL ROBINSON*

*Purdue University, Cytometry Laboratories, Department of Basic Medical Sciences, West Lafayette, IN, USA; and †Center for Immunology and Microbial Disease, Albany Medical College, Albany, NY, USA

(*Received* 9 *August* 2002; *Revised* 23 *September* 2002; *Accepted* 31 *October* 2002)

**Abstract**—The iodonium compounds diphenyleneiodonium (DPI) and diphenyliodonium (IDP) are well-known phagocyte NAD(P)H oxidase inhibitors. However, it has been shown that at high concentrations they can inhibit the mitochondrial respiratory chain as well. Since inhibition of the mitochondrial respiratory chain has been shown to induce superoxide production and apoptosis, we investigated the effect of iodonium compounds on mitochondria-derived superoxide and apoptosis. Mitochondrial superoxide production was measured on both cultured cells and isolated rat-heart submitochondrial particles. Mitochondria function was examined by monitoring mitochondrial membrane potential. Apoptotic pathways were studied by measuring cytochrome *c* release and caspase 3 activation. Apoptosis was characterized by detecting DNA fragmentation on agarose gel and measuring propidium iodide- (PI-) stained subdiploid cells using flow cytometry. Our results showed that DPI could induce mitochondrial superoxide production. The same concentration of DPI induced apoptosis by decreasing mitochondrial membrane potential and releasing cytochrome *c*. Addition of antioxidants or overexpression of MnSOD significantly reduced DPI-induced mitochondrial damage, cytochrome *c* release, caspase activation, and apoptosis. These observations suggest that DPI can induce apoptosis via induction of mitochondrial superoxide. DPI-induced mitochondrial superoxide production may prove to be a useful model to study the signaling pathways of mitochondrial superoxide. © 2003 Elsevier Science Inc.

**Keywords**—Apoptosis, Reactive oxygen species, Diphenyleneiodonium, Hydroethidine, JC-1, MnSOD, Mitochondrion, Free radicals

## INTRODUCTION

Reactive oxygen species (ROS) are a family of small but highly reactive molecules, including singlet oxygen, superoxide anion, hydrogen peroxide, organic peroxide radicals, and nitric oxide. ROS can be produced in vivo by many enzyme systems, including NADPH oxidase [1,2], NADH oxidase [3], xanthine oxidase [4], 5-lipoxygenase [5], and others. Under physiological conditions, the mitochondrial respiratory chain is the major site for ROS production in cells [6,7]. Based on studies in isolated mitochondria, about 1 to 2% of the oxygen consumed by the respiratory chain can be converted to ROS in the mitochondria [7]. In the presence of respiratory chain inhibitors such as the complex I inhibitor rotenone, N-methyl-4-phenylpyridinium, and the complex III inhibitor antimycin, levels of mitochondrial respiratory chain-derived ROS can be further elevated [8–10]. In mitochondria, manganese superoxide dismutase is the major enzyme responsible for converting superoxide to hydrogen peroxide [11–13]. Thus, it is of interest to focus on the role of various agents at the level of mitochondrial ROS production.

Recent evidence suggests that ROS may act as important regulators of apoptosis. Previous studies have shown that oxidants or pro-oxidants can induce apoptosis, while antioxidants can block or delay apoptosis [14–20]. On the other hand, many apoptotic stimuli, such as TNF-$\alpha$, UV radiation, ceramide, staurosporine, growth factor withdrawal, serum deprivation, human immunodeficiency virus infection, and environmental toxin exposure, have been shown to stimulate ROS production [21–29]. Mitochondrial ROS play an important role in apoptosis because mitochondrial ROS can readily influ-

Address correspondence to: Dr. J. Paul Robinson, Purdue University, Cytometry Laboratories, 201 South University Drive, West Lafayette, IN 47907, USA; Tel: (765) 494-0757; Fax: (765) 494-0517; E-Mail: jpr@flowcyt.cyto.purdue.edu.

ence mitochondrial function without having to diffuse a long way from the cytosol [30–33]. Several studies have demonstrated that overexpression of mitochondrial manganese superoxide dismutase is able to suppress apoptosis induced by a broad range of stimuli including TNF-$\alpha$ [34], alkalinity [35], peroxynitrite [36], and antimycin [37], indicating that mitochondrial superoxide was involved in these systems. However, due to the difficulty of tracing ROS in mitochondria, direct detection of mitochondrial ROS has not been possible in many systems. In addition, since extracellular or cytosolic ROS have also been shown to impair mitochondrial function, making it difficult to exclude the possible involvement of extramitochondrial ROS, the signaling pathways of mitochondrial ROS during apoptosis are still elusive.

Diphenyleneiodonium (DPI) and diphenyliodonium (IDP) are well-known inhibitors of flavoprotein oxidoreductases. They have been reported to inhibit phagocyte NADPH oxidase [38], nitric oxide synthase [39], xanthine oxidase [40], P-450 NADPH reductase [41], and mitochondrial respiratory chain complex I NADH reductase [42]. It has been suggested that both DPI and IDP form phenol radicals that attack a wide range of targets, including reduced flavin (FAD or FMN) of NADPH oxidase or P-450 reductase [38,41], heme component of NADPH oxidase [38], or iron-sulfur clusters in mitochondria complex I [43]. Since it has been suggested that a flavoprotein might be involved in superoxide production downstream of the Ras pathway, DPI and IDP have been used widely to inhibit cellular superoxide production and to inhibit apoptosis in many instances [44–46]. However, due to their inhibitory effect on mitochondria respiratory chain complex I [47], the iodonium compounds also have the potential to increase the production of superoxide and influence mitochondria function. Since the role of these so-called "ROS inhibitors" has not been well investigated, we carried out a detailed investigation of the effects of iodonium compounds on mitochondrial superoxide production in the present study. Our results demonstrated a clear and effective induction of mitochondrial superoxide production by DPI. Using this model, we have provided evidence that mitochondrial superoxide can directly induce apoptosis through decreasing mitochondrial membrane potential and release of cytochrome *c*.

## EXPERIMENTAL PROCEDURES

### *Cell culture and reagents*

Antihuman caspase 3 antibody and antihuman cytochrome *c* antibody were obtained from Santa Cruz Biotechnology, Inc. (Santa Cruz, CA, USA); 5,5',6,6'-tetrachloro-1,1',3,3'-tetraethylbenzimidazolylcarbocyanine iodide (JC-1), Hoechst 33342, and propidium iodide (PI) were obtained from Molecular Probes (Eugene, OR, USA); and, hydroethidine was obtained from Polysciences (Warrington, PA, USA). All other reagents, if not stated, were obtained from Sigma Chemical Co. (St. Louis, MO, USA).

The human promyelocytic leukemia cell line HL-60 was obtained from American Type Culture Collection (Manassas, VA, USA). Cells were cultured in RPMI-1640 medium supplemented with 10% fetal calf serum (FCS) and 2 mM L-glutamine. HL-60 cells deficient in mitochondrial DNA ($\rho^0$) were generated by growing HL-60 cells in RPMI-1640 medium supplied with 10% FCS, 2 mM L-glutamine, 1 mM pyruvate, 50 $\mu$g/ml uridine, 25 mM glucose, and 50 ng/ml ethidium bromide for 8 weeks, as previously described [48]. After selection, the cells were grown in the same medium without ethidium bromide. Oxygen consumption was measured with a clark-type oxygen electrode and no oxygen uptake was observed for $\rho^0$ HL-60 cells.

The human fibrosarcoma cell line HT-1080 (American Type Culture Collection) was maintained in DMEM containing 10% heat-inactivated FCS supplemented with 2 mM L-glutamine, 1 mM sodium pyruvate, and 100 units/ml penicillin. Construction of a stable HT-1080 cell line overexpressing magnesium superoxide dismutase (MnSOD) was previously described in detail [49]. HT-1080 cells stably transfected with MnSOD were maintained in medium that included 1 mg/ml G418 in addition to the above-mentioned supplements. All cell lines were cultured at 37°C with 5% $CO_2$.

### *Measurement of reactive oxygen species production in intact cells*

Measurement of superoxide in HL-60 cells was performed as described previously, with some modifications [50]. Cells were washed with Hank's balanced salt solution (HBSS), pelleted, and resuspended in HBSS containing 10 $\mu$M hydroethidine (HE). After 10 min incubation at 37°C, the cell suspension was placed into 12 $\times$ 75 mm tubes for assay. All studies were carried out on either an EPICS Elite flow cytometer (Beckman-Coulter Corp., Hialeah, FL, USA) using an air-cooled 15 mW argon laser (Cyonics Model 2201, San Jose, CA, USA) operating at a wavelength of 488 nm or a Coulter XL cytometer (Beckman-Coulter Corp.). Ethidium fluorescence was collected using a 610 nm long-pass filter.

### *Isolation of mitochondria, preparation of submitochondrial particles (SMPs), and measurement of mitochondrial superoxide production*

Rat-heart mitochondria were isolated by differential centrifugation as described by Lash and Sall [51], with some modifications. Briefly, rat hearts were obtained

from healthy young adult male Sprague Dawley (SD) rats. Pieces of heart were homogenized by a Dounce homogenizer in an isolation solution containing 250 mM sucrose, 10 mM HEPES, 1 mM EDTA, and 50 mg/ml nagarse, pH 7.4, at 4°C. The homogenate was centrifuged at 600 × *g* for 10 min, and the supernatant was collected and centrifuged again at 17,500 × *g*. The resulting mitochondrial pellet was washed and resuspended in isolation solution. To obtain SMPs, mitochondrial suspension was sonicated at 4°C with a 30 s pulse burst three times at 1 min intervals. The sonicated mitochondria were centrifuged at 8250 × *g* for 10 min, and the supernatant was centrifuged again at 80,000 × *g* at 4°C for 45 min. The resulting pellet was resuspended in isolation solution without EDTA. The amount of protein in the SMP suspension was determined by the Bradford method. NADH-dependent superoxide production was measured using an epinephrine-based assay on a Perkin-Elmer 3B double-beam spectrophotometer. The reaction was initiated by adding 1 mM NADH to the reaction chamber in the presence of 1 mM epinephrine. The superoxide concentration was estimated by measuring the absorbance of adrenochrome at 480 nm [9].

*Assessment of mitochondrial membrane potential change ($\Delta\Psi_m$)*

Mitochondrial membrane potential change was examined using the mitochondrial membrane potential-sensitive fluorescent dye 5,5',6,6'-tetrachloro-1,1',3,3'-tetraethylbenzimidazolylcarbocyanine iodide (JC-1). Cells were collected, pelleted, washed, and resuspended in PBS containing 2.5 μg/ml JC-1. Cells were kept in the dark at room temperature for 20 min. After loading, the cells were washed twice with PBS and analyzed by flow cytometry (excitation at 488 nm, with a 525 nm bandpass filter to collect green emission and a 590 nm bandpass filter to collect orange emission).

*Subcellular fractionation*

Approximately $1 \times 10^7$ cells were collected, washed once with PBS, and then resuspended in a buffer containing 250 mM sucrose, 10 mM HEPES, 1 mM EDTA, 10 μg/ml aprotinin, 10 μg/ml leupeptin, 1 mM PMSF, 1 mM dithiothreitol, and 1 mM sodium orthovanadate, pH 7.4, at 4°C. Digitonin (400 ng/ml) was then added to the cell suspension and lysis of cells confirmed under the microscope. After centrifugation at 12,000 × *g* for 15 min at 4°C, cell lysates were transferred to fresh tubes and used as cytosol components.

*Whole cell extraction*

Approximately $1 \times 10^7$ cells were harvested and washed once with ice-cold PBS, resuspended in 1 ml ice-cold lysis buffer containing 1% Nonidet P-40, 20 mM Tris-HCl (pH 8.0), 10% glycerol, 137 mM NaCl, 2 mM EDTA, 10 μg/ml aprotinin, 10 μg/ml leupeptin, 1 mM PMSF, and 1 mM sodium orthovanadate, and incubated on ice for 30 min. After centrifugation at 10,000 × *g* for 10 min at 4°C, cell lysates were transferred to fresh tubes and stored at −80°C.

*Western blotting*

Cell homogenates (50 μg protein) were fractionated by SDS-PAGE on a 15% acrylamide gel. Bands of proteins were then transferred to a PVDF membrane (Bio-Rad, Hercules, CA, USA). The PVDF membrane was blocked by 5% milk overnight at 4°C and then incubated with antibodies against either cytochrome *c* or caspase 3 for 3 h at room temperature. After an additional 1 h incubation with horseradish peroxidase-conjugated secondary antibodies, the binding of antibodies to the PVDF membrane was detected with an enhanced chemiluminescence western blotting analysis (Amersham Pharmacia Biotech, Buckinghamshire, England).

*Measurement of apoptosis*

Degradation of DNA was measured by flow cytometry, confocal microscopy, and agarose gel electrophoresis. For flow cytometric analysis, propidium iodide (PI) was used to detect DNA breakdown, as described previously. Cells were collected and fixed in suspension in 70% ethanol on ice and then stored at −20°C for at least 4 h. Cells were centrifuged at 500 × *g*, washed with 5 ml HBSS, centrifuged again, and resuspended in 1 ml HBSS. After addition of 0.2 ml phosphate citrate buffer (pH 7.8), cells were incubated at room temperature for 5 min before being washed again and resuspended in HBSS containing 20 μg/ml PI and 10 μg/ml RNase A. After 30 min incubation in the dark at room temperature, PI fluorescence was analyzed by flow cytometry.

Apoptosis was also measured by observing morphological changes in the nuclear chromatin of cells detected by staining with 2 μg/ml Hoechst 33342, followed by examination on a Bio-Rad MC 1024-UV confocal microscope.

The DNA fragmentation assay was performed according to the method described previously [52], with some modifications. HL-60 cells were washed twice with PBS (4°C, pH 7.4) and collected by centrifugation at 500 × *g* for 5 min. Cell concentration was adjusted to $2 \times 10^7$/ml. After centrifugation at 500 × *g*, cells were treated with 0.5 ml lysis buffer (10 mM Tris-HCl, pH 7.4, 10 mM EDTA, 0.5% sodium dodecyl sulfate) for 10 min on ice. After treatment with RNase A (final concentration 100 μg/ml) for 1 h at 37°C, the cells were incubated at 50°C for 4 h in the presence of 100 μg/ml proteinase K. DNA

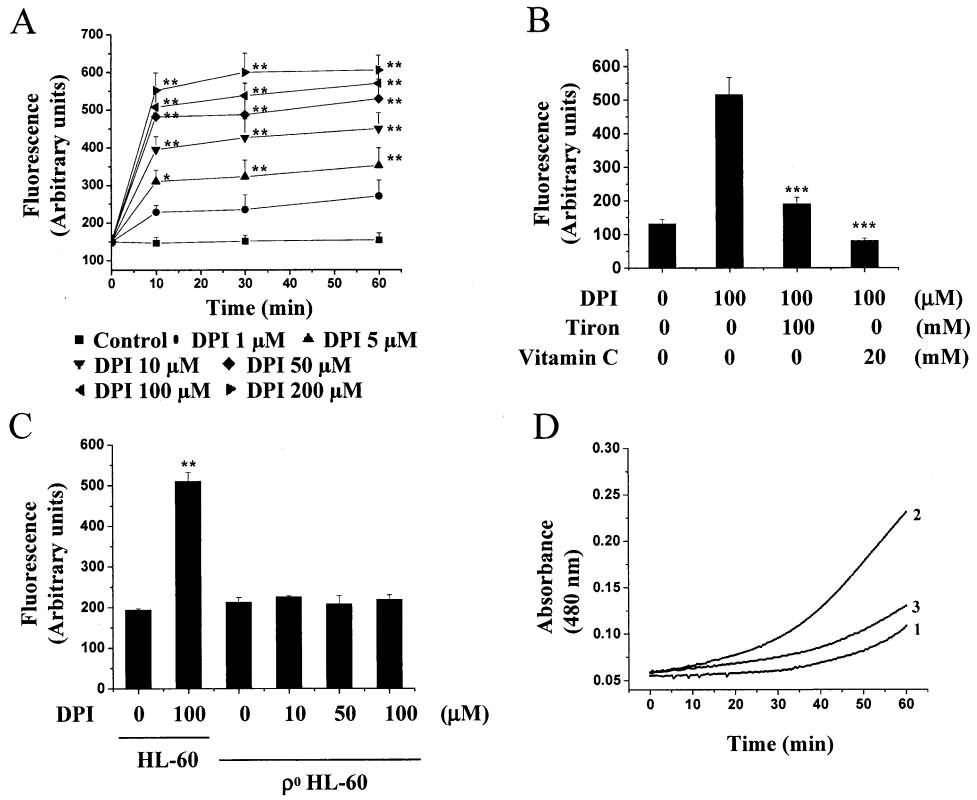


Fig. 1. Diphenyleneiodonium (DPI)-induced reactive oxygen species (ROS) production. Cells were treated with DPI for the time indicated in each figure. Cellular ROS production was estimated by the increase of ethidium fluorescence based on flow cytometry assays. (A) Cellular ROS production in HL-60 cells treated with various concentrations of DPI for different times as indicated. (B) HL-60 cells pretreated with either 100 mM Tiron or 20 mM vitamin C for 10 min. DMSO or DPI, 100 $\mu$M in DMSO, was then added to the medium and incubated for 1 h. Cellular ROS production was measured by flow cytometry. (C) Cellular ROS production in HL-60 cells or mitochondrial DNA-deficient ($\rho^0$) HL-60 cells treated with various concentrations of DPI for 1 h as indicated. (D) DPI induced an NADH-based mitochondrial superoxide production on submitochondrial particles. Rat-heart submitochondrial particles were incubated with: 1, nothing (Control); 2, DPI (100 $\mu$M); 3, DPI (100 $\mu$M) and SOD (100 units). Superoxide production was measured by conversion of epinephrine to adrenochrome. The absorbance of adrenochrome was monitored at 480 nm. Results are representative ones from three separate experiments. Significant difference from control group (for A and B) or from DPI-only group (for C) at $*p < .05$, $**p < .01$, and $***p < .001$.

was then precipitated with 50 $\mu$l of 3 M sodium acetate (pH 5.2) and 1 ml cold (4°C) 100% ethanol. Finally, DNA was dissolved in Tris-EDTA. For analysis, 10 to 20 $\mu$l DNA was loaded on a 1.2% agarose gel containing 10 $\mu$g/ml ethidium bromide. Electrophoresis was performed in 0.5 × Tris-Borate-EDTA buffer at 70 V for 2 h. DNA was visualized under ultraviolet light and imaged.

## RESULTS

### *Diphenyleneiodonium (DPI) induces superoxide production in mitochondria*

HL-60 cells were used as the model to study the effect of DPI on cellular superoxide production. The conversion of hydroethidine to ethidium was used as a measurement of superoxide production. Hydroethidine has been used to identify superoxide in a number of systems [53–55] and has also been shown to be superoxide specific [56–58], though there are potential complications in using this dye [59]. DPI concentrations of 1–200 $\mu$M increased the cellular ethidium fluorescence in a dose-dependent manner after 10 min (Fig. 1A). Longer treatments did not result in further increases in ethidium fluorescence, indicating that the velocity of cellular superoxide production did not further increase. When HL-60 cells were pretreated with the antioxidant 4,5-dihydroxy-1,3-benzene-disulfonic acid (Tiron; Sigma Chemical Co.) or vitamin C, the DPI-induced cellular ethidium fluorescence increase measured 1 h after DPI treatment was inhibited (Fig. 1B).

To further investigate whether DPI-induced superoxide production was from mitochondria, HL-60 cells that lack mitochondrial DNA ($\rho^0$) were treated with various concentrations of DPI and then loaded with hydroethi-

dine. DPI could not elevate ethidium fluorescence in $\rho^0$ HL-60 cells after treatment for 1 h (Fig. 1C), although ethidium fluorescence increased when normal HL-60 cells were treated with DPI for the same length of time (Fig. 1C).

Finally, the conversion of epinephrine to adrenochrome was used to measure superoxide production on isolated rat-heart submitochondrial particles (Fig. 1D). For the controls, the increase of absorbance at 480 nm was less than 0.05 within 1 h. DPI in the absence of submitochondrial particles showed no increase in absorbance (data not shown). For SMPs in the presence of 100 $\mu$M DPI, the absorbance at 480 nm was significantly increased. The presence of superoxide dismutase inhibited the increased absorbance induced by DPI.

*DPI induces apoptosis in HL-60 cells*

We examined the effect of DPI on apoptosis using HL-60 cells. Apoptosis was studied by confocal microscopy using Hoechst 33342 and by flow cytometry using propidium iodide (PI). For flow cytometry assays, HL-60 cells were incubated with DPI, fixed, and permeabilized. The cells were then loaded with 20 $\mu$g/ml PI and their DNA content was analyzed by flow cytometry. Incubation of HL-60 cells with 50–100 $\mu$M DPI for 12 h led to the appearance of subdiploid cells (Fig. 2). For confocal microscopy, HL-60 cells were treated with DPI and then loaded with 2 $\mu$g/ml Hoechst 33342 for 20 min at 37°C. Nuclear condensation and fragmentation of DPI-treated HL-60 cells were clearly visible under the confocal microscope, as was the higher intensity of blue fluorescence from the nuclei (Fig. 2). Finally, genomic DNA of DPI-treated HL-60 cells was collected and run on 1% agarose gel electrophoresis. DNA ladders were observed after 24 h treatment with 50–100 $\mu$M DPI (Fig. 3A).

The number of subdiploid cells in DNA ploidy analysis was calculated using flow cytometry to estimate the degree of apoptosis. Cellular toxicity of DPI was dependent on both the concentration and the time of exposure. After a 12 h incubation with 100 $\mu$M DPI, more than 70% of the cells were apoptotic (Fig. 3B).

To investigate the role of mitochondrial superoxide in DPI-induced apoptosis, HL-60 cells were incubated with either Tiron or vitamin C before DPI treatment. Both Tiron and vitamin C pretreatments resulted in the inhibition of DPI-induced apoptosis at 12 h (Fig. 3C).

To determine the effect of caspase inhibitors on DPI-induced apoptosis, HL-60 cells were incubated with 100 $\mu$M DPI in the presence or absence of either 25 $\mu$M z-VAD-FMK or 25 $\mu$M Ac-DEVD-CHO. As demonstrated in Fig. 4, z-VAD-FMK and Ac-DEVD-CHO both decreased the subdiploid population of DPI-treated HL-60 cells at 12 h.

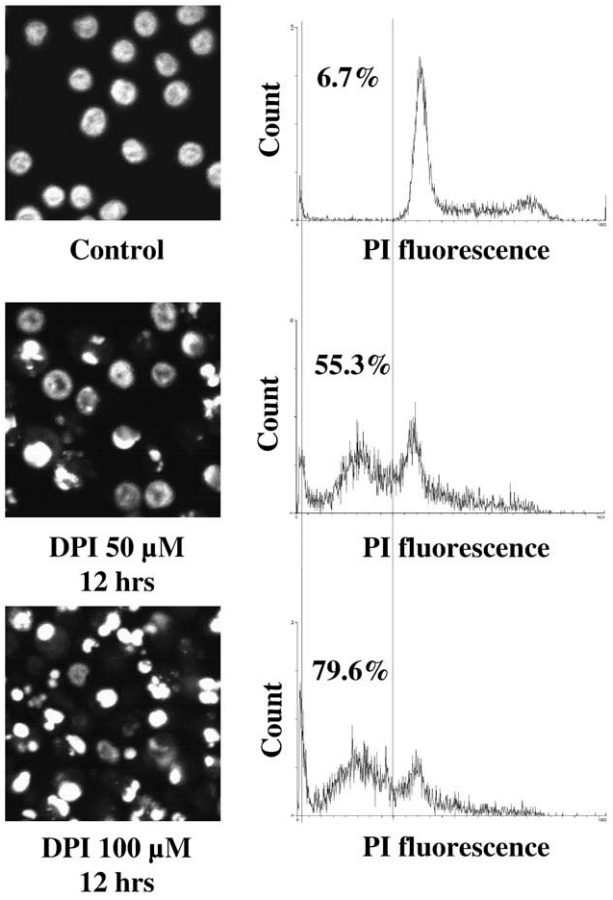


Fig. 2. DPI-induced apoptosis in HL-60 cells. HL-60 cells were incubated with either DMSO (control) or DPI, 50–100 $\mu$M in DMSO (as indicated), for 12 h. Left panel: cells stained with Hoechst 33342 and photographed under the confocal microscope. Right panel: cells fixed and stained with PI. Cell cycle analysis was performed by flow cytometry. Apoptotic cells were estimated by calculating the number of subdiploid cells in the cell cycle histogram. The numbers in each panel refer to the percentage of apoptotic cells. Results are representative of three separate experiments.

*DPI induces mitochondrial depolarization*

We examined the effect of DPI on mitochondrial membrane potential to clarify the pathway involved in DPI-induced apoptosis. HL-60 cells were treated with different concentrations of DPI for different time intervals and then loaded with JC-1. The JC-1 fluorescence was measured by flow cytometry at both 525 and 590 nm. The number of cells that lost mitochondrial membrane potential was estimated by calculating the changes in percentage expression in the fourth quadrant, which represents cells having both reduced 590 nm and increased 525 nm fluorescence (Fig. 5A). Valinomycin (100 nM) (Sigma Chemical Co.) was used as a positive control for mitochondrial depolar-

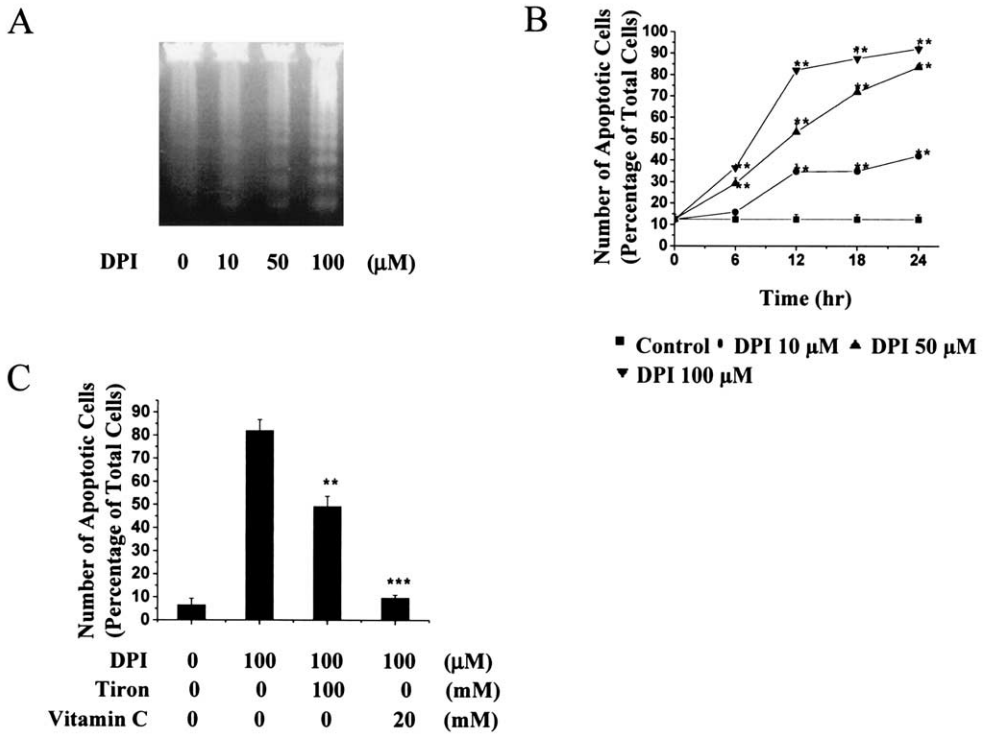


Fig. 3. DPI-induced apoptosis in HL-60 cells. (A) DPI-induced DNA fragmentation. HL-60 cells were treated with indicated concentrations of DPI for 12 h. Genomic DNA was isolated, run on a 1% agarose gel, and visualized by ethidium bromide staining. Results are representative of three separate experiments. (B) After treatment with various concentrations of DPI for different times as indicated, HL-60 cells were fixed and cell cycle analysis was performed by flow cytometry. Number of apoptotic cells was estimated by calculating the number of subdiploid cells. (C) Inhibition of DPI-induced apoptosis by antioxidants. HL-60 cells were treated with 100 $\mu$M DPI in the presence or absence of 100 mM Tiron or 20 mM vitamin C. Cells were fixed and cell cycle analysis was performed by flow cytometry. Number of apoptotic cells was estimated by calculating the number of subdiploid cells. Significant difference from control group at $*p < .05$, $**p < .01$, and $***p < .001$.

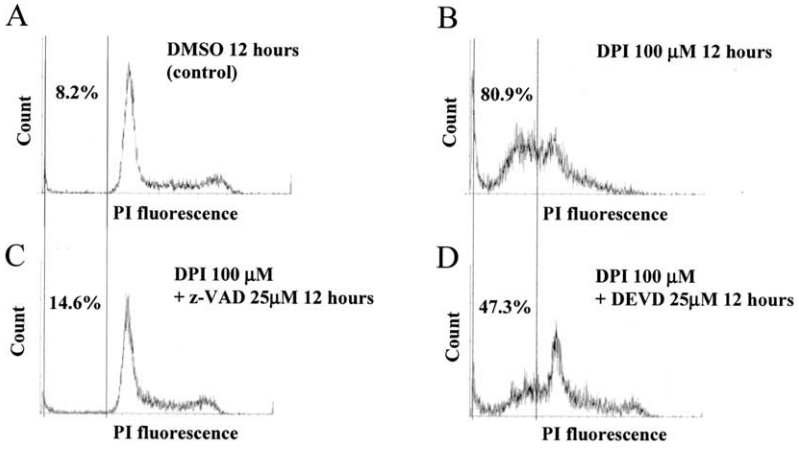


Fig. 4. Inhibition of DPI-induced apoptosis by caspase inhibitors z-VAD and DEVD. HL-60 cells were incubated with (A) DMSO (control), (B) DPI (100 $\mu$M), (C) DPI (100 $\mu$M) and z-VAD (25 $\mu$M), and (D) DPI (100 $\mu$M) and DEVD (25 $\mu$M), for 12 h. Cells were fixed and stained with PI. Cell cycle analysis was performed by flow cytometry. Apoptotic cells were estimated by calculating the number of subdiploid cells in the cell cycle histogram. The number in each panel refers to the percentage of apoptotic cells. Results are representative of three separate experiments.

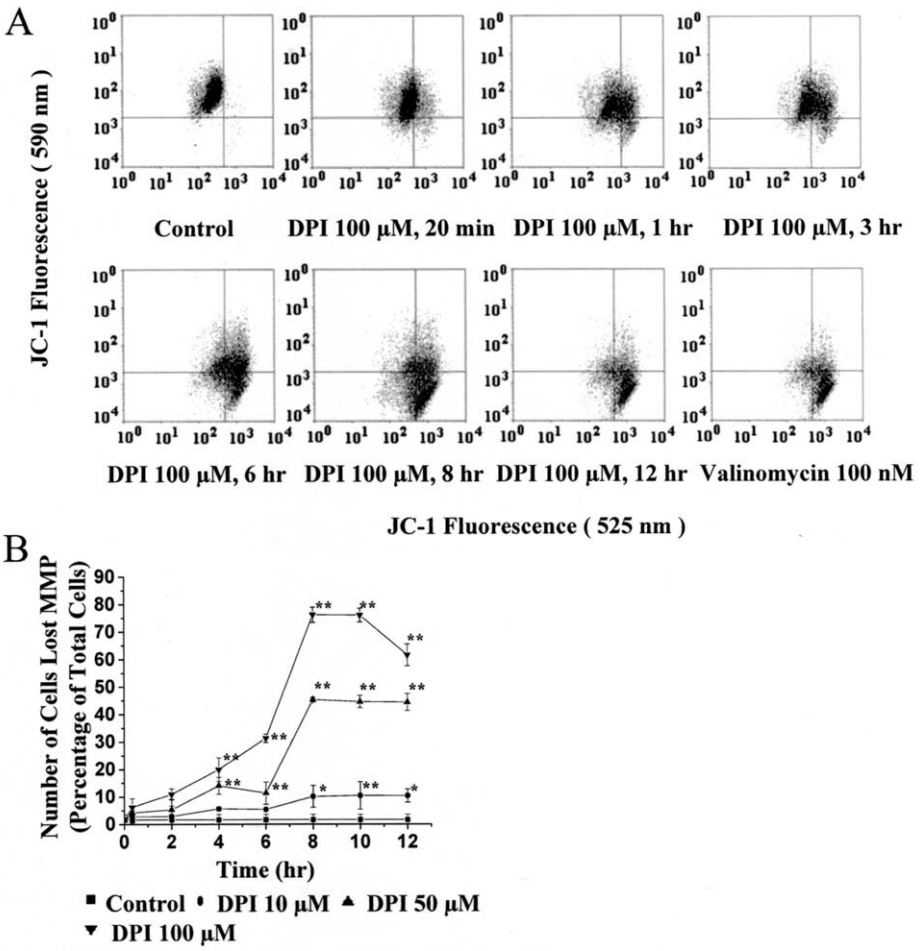


Fig. 5. DPI-induced loss of mitochondrial membrane potential in HL-60 cells. Mitochondrial membrane potential was studied by flow cytometry using JC-1. (A) HL-60 cells were treated with 100 $\mu$M DPI for different lengths of time (20 min to 12 h), and valinomycin (100 nM) was used to entirely abolish mitochondrial membrane potential. Results are representative of three separate experiments. (B) Time-course study of DPI-induced decrease of mitochondrial membrane potential in HL-60 cells. Cells were treated with various concentrations of DPI for the indicated times. Cells in the fourth quadrant were counted as cells deprived of mitochondrial membrane potential. Significant difference from control group at $*p < .05$ and $**p < .01$.

ization. HL-60 cells treated with 100 $\mu$M DPI showed an initial decrease in mitochondrial membrane potential 2 h after treatment (Figs. 5A and 5B). Within 6 h, DPI-treated HL-60 cells underwent a slow but gradual decrease of mitochondrial membrane potential. Most cells lost mitochondrial membrane potential by 8 h after 100 $\mu$M DPI treatment. DPI diminished the mitochondrial membrane potential in a dose-dependent manner (Fig. 5B). To determine the effect of antioxidants on DPI-induced mitochondrial membrane potential, HL-60 cells were preincubated with either 100 mM Tiron or 20 mM vitamin C before DPI treatment. Both reagents reduced the number of cells that lost mitochondrial membrane potential after 8 h of DPI treatment (Figs. 6A and 6B).

*DPI induces cytochrome c release and caspase 3 activation*

We studied the effect of DPI on HL-60 cytochrome *c* release by western blot. After treatment of HL-60 cells with 50–100 $\mu$M DPI for 6 h, cytochrome *c* was released to the cytosol (Fig. 7A). Release of cytochrome *c* by DPI reached a peak after 8 h treatment, and did not increase further thereafter. The release of cytochrome *c* by DPI is not dose dependent, consistent with other reports that cytochrome *c* release is a "rapid, complete, and kinetically invariant" process [60]. Caspase 3 activation induced by DPI was also measured by western blot. Consistent with cytochrome *c* release, caspase 3 was activated after 6 h of DPI treatment (Fig. 7B). Maximum caspase 3 activation was detected after 8–10 h treatment

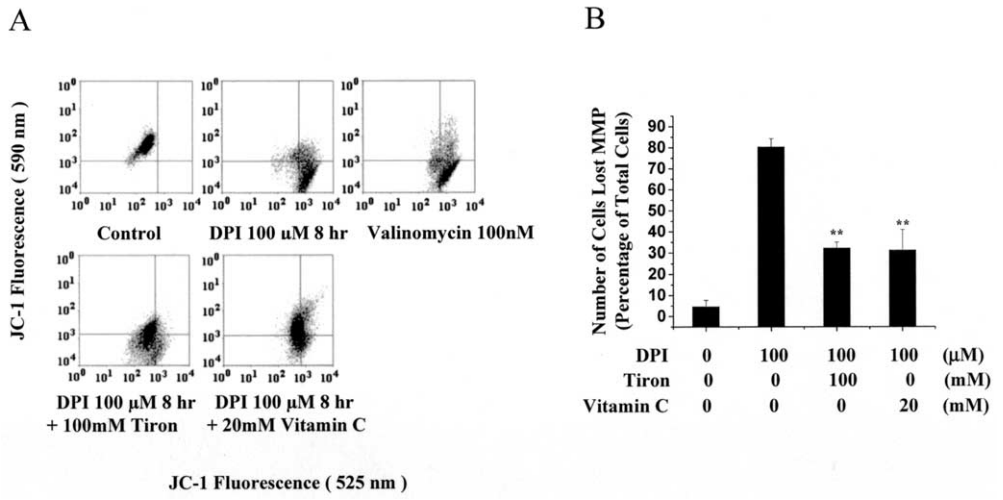


Fig. 6. Inhibition of DPI-induced mitochondrial membrane potential loss by Tiron and vitamin C. (A) HL-60 cells were pretreated with either 100 mM Tiron or 20 mM vitamin C for 10 min; 100 $\mu$M DPI was then added to the medium. After 8 h, HL-60 cells were harvested and mitochondrial membrane potential was analyzed by flow cytometry using JC-1. Results are representative of three separate experiments. (B) Inhibition of DPI-induced decrease of mitochondrial membrane potential by either 100 mM Tiron or 20 mM vitamin C. Cells in the fourth quadrant were counted as cells deprived of mitochondrial membrane potential. Significant difference from control group at $^{**}p < .01$.

with DPI. Preincubation of HL-60 cells with either Tiron or vitamin C inhibited the release of cytochrome *c* and activation of caspase 3 by DPI at 8 h (Figs. 8A–8D).

### *Mitochondrial magnesium superoxide dismutase (MnSOD) overexpression inhibits DPI-induced superoxide production, decrease of mitochondrial membrane potential, and DNA breakdown*

To confirm that DPI induces apoptosis through mitochondrial-derived superoxide, we tested the effect of DPI on an HT-1080 fibrosarcoma cell line that was transfected with either empty vector or a vector containing the open reading frame of human MnSOD (CMV = control transfectants, HT15 = cells with 15-fold increase in MnSOD levels). All cells were treated with DPI and loaded with hydroethidine as described earlier. The conversion of hydroethidine to ethidium was used as a measurement of superoxide production. The basal ethidium fluorescence of HT15 cells was lower than that of CMV cells, indicating that the cells overexpressing MnSOD demonstrate a lower superoxide production (Fig. 9A). As indicated by the elevated ethidium fluorescence, DPI increased superoxide production in both CMV and HT15 cells. However, for all DPI concentrations, ethidium fluorescence was about 50% lower in the HT15 cells compared to CMV cells (Fig. 9A). Previous reports showed the validity of using hydroethidine to probe intramitochondria superoxide production [61].

The effect of DPI on mitochondrial membrane potential was also measured on both CMV and HT15 cells. All untreated cells (CMV and HT15) maintained mitochondrial membrane potential, as shown in Fig. 9B. After an 8 h treatment with 100 $\mu$M DPI, 40% of CMV cells localized to the fourth quadrant, indicating loss of mitochondrial membrane potential. However, only 13% of HT15 cells were located in the fourth quadrant (Figs. 9B

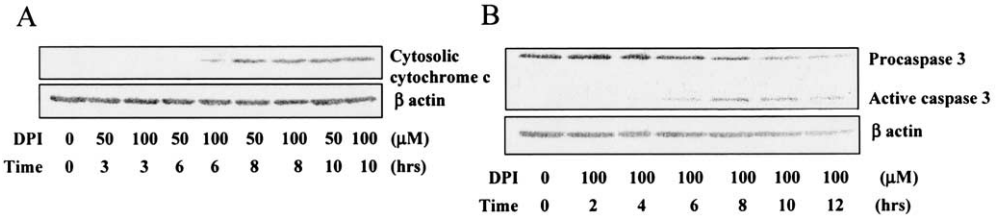


Fig. 7. DPI-induced cytochrome *c* release and caspase 3 activation. (A) Time-course study of DPI-induced cytochrome *c* release. HL-60 cells were treated with 50–100 $\mu$M DPI for various times as indicated. Cytosol cytochrome *c* level was determined by western blot analysis. (B) Time-course study of DPI-induced activation of caspase 3 activation. HL-60 cells were treated with 50–100 $\mu$M DPI for various times as indicated. Caspase 3 level was determined by western blot analysis. Results are representative of three separate experiments.

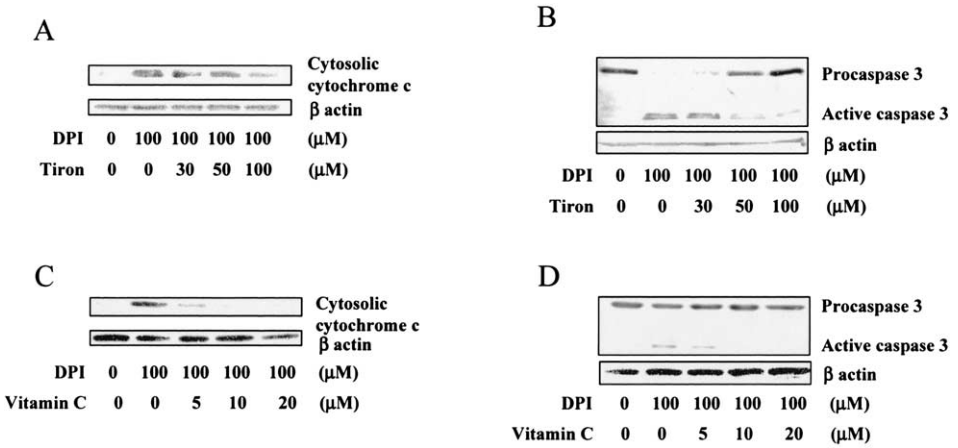


Fig. 8. Inhibition of DPI-induced cytochrome *c* release and caspase 3 activation by antioxidants. HL-60 cells were pretreated with various concentrations of Tiron or vitamin C. Cells were then incubated with 100 $\mu$M DPI for 8 h. Cytosol cytochrome *c* or caspase 3 was detected by western blot. (A) Inhibition of DPI-induced cytochrome *c* release by Tiron. (B) Inhibition of DPI-induced caspase 3 activation by Tiron. (C) Inhibition of DPI-induced cytochrome *c* release by vitamin C. (D) Inhibition of DPI-induced caspase 3 activation by vitamin C. All results are representative of three separate experiments.

and 9C). Valinomycin depleted mitochondrial membrane potential in both cell types (Fig. 9B).

The impact of MnSOD overexpression on DPI-induced apoptosis was also examined. The number of subdiploid cells in DNA ploidy analysis was used as an estimate of the degree of apoptosis. The percentage of both cell types undergoing apoptosis increased after incubation with 100 $\mu$M DPI (Fig. 10). After a 24 h

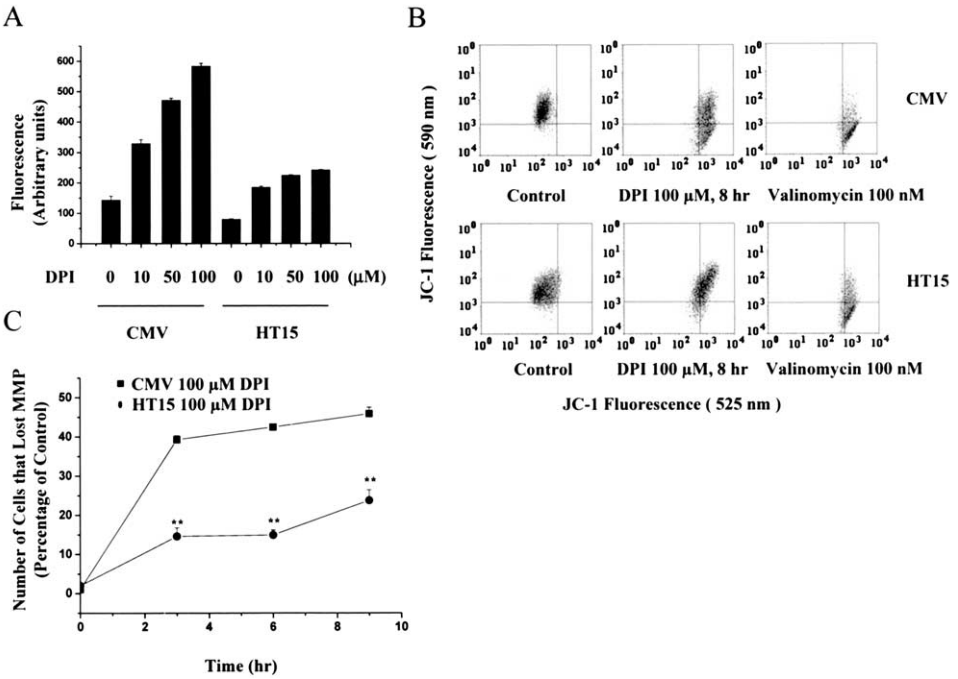


Fig. 9. Inhibition of DPI-induced superoxide production and mitochondrial membrane potential decrease by MnSOD overexpression. HT-1080 fibrosarcoma cell line was transfected with either empty vector or a vector containing the open reading frame of human MnSOD (CMV = control transfectants, HT15 = cells with 15-fold increase in MnSOD levels). (A) Cells were treated with various concentrations of DPI for 1 h and then collected. Cellular ROS production was estimated by the increase of ethidium fluorescence based on flow cytometric assays. (B and C) Cells were treated with 100 $\mu$M DPI. Mitochondrial membrane potential was studied by flow cytometry using JC-1. Cells in the fourth quadrant were counted as cells deprived of mitochondrial membrane potential. Results are representative of three separate experiments. Significant difference from control group at $^{**}p < .01$.

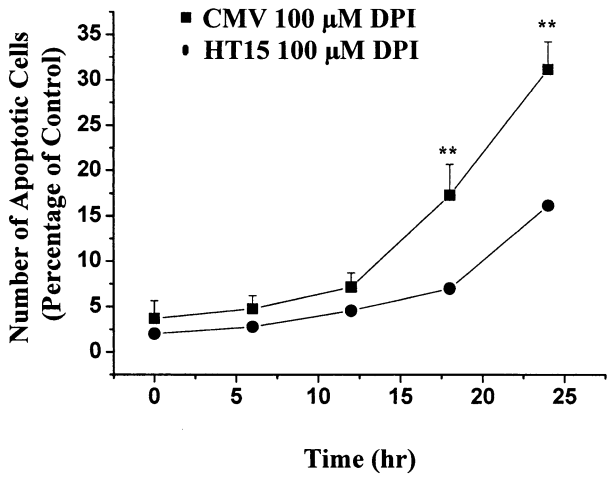


Fig. 10. Inhibition of DPI-induced apoptosis by MnSOD overexpression. CMV and HT15 cells were treated with 100 $\mu$M DPI for different lengths of time as indicated. The number of apoptotic cells was assessed by counting subdiploid cells using flow cytometry. Significant difference from control group at $^{**}p < .01$.

treatment with 100 $\mu$M DPI, more than 30% of CMV cells were apoptotic. However, in HT15 cells, the same concentration of DPI caused only 15% of the cells to become apoptotic (Fig. 10).

## DISCUSSION

In the present study, we showed that the flavoprotein inhibitor diphenyleneiodonium could induce mitochondrial reactive oxygen species (ROS) production and apoptosis. This is the first demonstration that DPI is able to elevate mitochondrial ROS production via an inhibition of the mitochondrial respiratory chain. Furthermore, the elevated mitochondrial ROS are then able to induce apoptosis by initiating loss of mitochondrial membrane potential, cytochrome *c* release, and caspase activation.

We observed an elevation of cellular ROS production with DPI in all cells used in this study (except $\rho^0$ HL-60 cells). Flow cytometric study of individual cells to detect intracellular superoxide levels found that DPI stimulated superoxide production in HL-60 cells in a dose-dependent manner. The range of DPI concentration capable of inducing superoxide production approximates the concentration range previously reported for respiratory inhibition by this reagent. In addition, DPI was not able to induce superoxide production in mitochondrial DNA-deficient HL-60 ($\rho^0$) cells, indicating the involvement of mitochondria in DPI-induced superoxide production. To further clarify that DPI-induced superoxide production was mitochondria related, we measured superoxide generation by rat-heart submitochondrial particles after DPI treatment. As expected, DPI was able to enhance the NADH-based superoxide production by submitochondrial particles. In addition, since previous studies have shown that the flavoprotein inhibitor DPI is able to inhibit a great variety of membrane-bound or cytosol superoxide-producing enzymes [38–41], possible involvement of these enzymes was excluded. Taken together, these results suggest that DPI can induce mitochondrial superoxide production through mitochondrial respiratory chain inhibition.

It is generally accepted that elevation of cellular ROS can promote apoptosis [14–20]. However, the detailed mechanisms are still elusive, partly because the site of ROS production during apoptosis is not clear. The mitochondrion is one of the most important ROS-producing sites in eukaryotic cells. It has long been suspected that mitochondrial ROS are involved in apoptosis following many stimuli, such as UV radiation, TNF-$\alpha$, and staurosporine [21,22,34]. However, the lack of mitochondrial ROS-producing models makes it difficult to clarify the role of mitochondrial ROS in apoptosis.

Since we have shown that DPI can induce mitochondrial ROS production, this reagent might provide a useful model for studying the role of mitochondrial ROS in apoptosis. We first examined whether DPI was able to induce apoptosis. Our results showed that, in HL-60 cells, DPI induced the appearance of subdiploid cells indicative of apoptotic cell death. Observations of nuclear condensation by confocal microscopy confirmed DPI-induced apoptotic cell death in HL-60 cells. In addition, agarose gel electrophoresis provided evidence of typical apoptotic DNA fragmentation patterns. Next, we studied the effect of antioxidants on DPI-induced apoptosis. Tiron (100 mM) and vitamin C (20 mM) were shown to inhibit DPI-induced superoxide production in HL-60 cells. It is possible that a reasonably high concentration of Tiron is required to facilitate the entry of this antioxidant into the mitochondrial component [62,63]. The same concentrations of Tiron and vitamin C were capable of inhibiting DPI-induced DNA breakdown at 12 h. Furthermore, fibrosarcoma HT-1080 cells overexpressing mitochondrial magnesium superoxide dismutase (HT15 cells) demonstrated less mitochondrial superoxide production than HT-1080 cells transfected with empty vector (CMV cells), and, as expected, more resistance to DPI-induced apoptotic cell death. All this evidence strongly suggests that mitochondrial ROS play a vital role in DPI-induced apoptosis.

To identify pathways that might be involved in DPI-induced apoptosis, we examined the effect of DPI on the decrease of mitochondrial membrane potential and release of cytochrome *c*, which are the two most important hallmarks of apoptotic cell death. The results presented in this study show that DPI could induce both a decrease in mitochondrial membrane potential and release of cy-

tochrome *c*. Decrease in mitochondrial membrane potential after DPI treatment was also shown to be the first event following mitochondrial superoxide production. This mitochondrial membrane potential decrease began approximately 1 to 2 h following the production of mitochondrial superoxide and continued for 2–6 h. The mechanism of this slow phase of mitochondrial membrane potential loss is not known. One possible explanation is the heterogeneous content of cellular antioxidants in the whole HL-60 cell population. This slow but continuous process might result from the loss of mitochondrial membrane potential in cells with lower mitochondrial antioxidant level. The mitochondrial membrane potential underwent rapid collapse after a 6 h treatment with DPI. The majority of cells were deprived of mitochondrial membrane potential after 8 h of treatment with 100 $\mu$M DPI.

Cytochrome *c* release and caspase 3 activation occurred about the same time as the collapse of mitochondrial membrane potential. These results indicate that the classical mitochondrial membrane potential loss, cytochrome *c* release, and caspase 3 activation pathway are the mechanisms for DPI-induced apoptosis. Our observations also demonstrated that both the decrease of mitochondrial membrane potential and the cytochrome *c* release occurred after mitochondrial ROS production. Therefore, the possibility reported by others using different apoptotic stimuli that ROS production could be caused by the disruption of mitochondrial membrane potential or release of cytochrome *c* was excluded in this system [42]. In addition, both mitochondrial membrane potential decrease and cytochrome *c* release in HL-60 cells were inhibited by Tiron and vitamin C. HT-1080 cells overexpressing MnSOD (HT15) were also more resistant than control cells to DPI-induced mitochondrial membrane potential loss, supporting the idea of this report that mitochondrial ROS induces apoptosis through the disruption of mitochondrial membrane potential and release of cytochrome *c*.

Once released from mitochondria to the cytosol, cytochrome *c* binds to the cytosol protein apaf-1 to activate caspase 9 [64]. Active caspase 9 directly activates caspase 3, which will finally lead to cell death [65]. Consistent with previous observations, our results showed the activation of caspase 3 immediately following the release of cytochrome *c*. Caspase 3 activation was inhibited both by caspase inhibitors and by antioxidants (Tiron and vitamin C). However, caspase inhibitors were not able to inhibit either cytochrome *c* release or decrease of mitochondrial membrane potential (data not shown). Our findings are consistent with previous results [64] that the activation of caspase 3 is downstream of mitochondrial membrane potential decrease and cytochrome *c* release.

A growing body of literature suggests that ROS play an important role in apoptosis. There is a considerable amount of evidence that cytosolic ROS are able to induce apoptosis [2,66]. In the present study, investigating the role of mitochondrial ROS in DPI-induced apoptosis, we showed that mitochondrial ROS could itself induce apoptosis via induction of mitochondrial membrane potential decrease, release of cytochrome *c*, and activation of caspase 3. This model might also be used to explain the mechanism of other apoptosis models, such as TNF-$\alpha$, ceramide, and ischemia, in which blocking of the mitochondrial respiratory chain have been reported [23,24,27].

DPI is well known as an NADPH oxidase inhibitor [38]. It was subsequently found that this reagent was capable of inhibiting most ROS-producing enzymes in the cell [39–41]. For this reason, DPI was frequently used as an antioxidant [44–46]. However, the present data suggest that DPI can act both as an antioxidant and also an inducer of mitochondrial superoxide production. Our data prompt a rethinking of some previously assumed pathways.

## REFERENCES


[1] Babior, B. M. NADPH oxidase: an update. *Blood* **93:**1464–1476; 1999.

[2] Bonizzi, G.; Piette, J.; Schoonbroodt, S.; Greimers, R.; Havard, L.; Merville, M. P.; Bours, V. Reactive oxygen intermediate-dependent NF-$\kappa$B activation by interleukin-1$\beta$ requires 5-lipoxygenase or NADPH oxidase activity. *Mol. Cell. Biol.* **19:**1950–1960; 1999.

[3] DeLeo, F. R.; Quinn, M. T. Assembly of the phagocyte NADPH oxidase: molecular interaction of oxidase proteins. *J. Leukoc. Biol.* **60:**677–691; 1996.

[4] Hille, R.; Nishino, T. Flavoprotein structure and mechanism. 4. Xanthine oxidase and xanthine dehydrogenase. *FASEB J.* **9:**995–1003; 1995.

[5] Morre, D. J.; Brightman, A. O. NADH oxidase of plasma membranes. *J. Bioenerg. Biomembr.* **23:**469–489; 1991.

[6] Barja, G. Mitochondrial oxygen radical generation and leak: sites of production in states 4 and 3, organ specificity, and relation to aging and longevity. *J. Bioenerg. Biomembr.* **31:**347–366; 1999.

[7] Boveris, A.; Chance, B. The mitochondrial generation of hydrogen peroxide. General properties and effect of hyperbaric oxygen. *Biochem. J.* **134:**707–716; 1973.

[8] Hasegawa, E.; Takeshige, K.; Oishi, T.; Murai, Y.; Minakami, S. 1-Methyl-4-phenylpyridinium (MPP+) induces NADH-dependent superoxide formation and enhances NADH-dependent lipid peroxidation in bovine heart submitochondrial particles. *Biochem. Biophys. Res. Commun.* **170:**1049–1055; 1990.

[9] Turrens, J. F.; Boveris, A. Generation of superoxide anion by the NADH dehydrogenase of bovine heart mitochondria. *Biochem. J.* **191:**421–427; 1980.

[10] Turrens, J. F.; Freeman, B. A.; Levitt, J. G.; Crapo, J. D. The effect of hyperoxia on superoxide production by lung submitochondrial particles. *Arch. Biochem. Biophys.* **217:**401–410; 1982.

[11] Boveris, A.; Cadenas, E. Mitochondrial production of superoxide anions and its relationship to the antimycin insensitive respiration. *FEBS. Lett.* **54:**311–314; 1975.

[12] Dionisi, O.; Galeotti, T.; Terranova, T.; Azzi, A. Superoxide radicals and hydrogen peroxide formation in mitochondria from

normal and neoplastic tissues. *Biochim. Biophys. Acta* **403:**292–300; 1975.

[13] Weisiger, R. A.; Fridovich, I. Superoxide dismutase. Organelle specificity. *J. Biol. Chem.* **248:**3582–3592; 1973.

[14] Chrestensen, C. A.; Starke, D. W.; Mieyal, J. J. Acute cadmium exposure inactivates thioltransferase (glutaredoxin), inhibits intracellular reduction of protein-glutathionyl-mixed disulfides, and initiates apoptosis. *J. Biol. Chem.* **275:**26556–26565; 2000.

[15] Fang, N.; Casida, J. E. Anticancer action of cube insecticide: correlation for rotenoid constituents between inhibition of NADH:ubiquinone oxidoreductase and induced ornithine decarboxylase activities. *Proc. Natl. Acad. Sci. USA* **95:**3380–3384; 1998.

[16] Heussler, V. T.; Fernandez, P. C.; Machado, J. Jr.; Botteron, C.; Dobbelaere, D. A. N-acetylcysteine blocks apoptosis induced by N-$\alpha$-tosyl-L-phenylalanine chloromethyl ketone in transformed T-cells. *Cell. Death Differ.* **6:**342–350; 1999.

[17] Kelso, G. F.; Porteous, C. M.; Coulter, C. V.; Hughes, G.; Porteous, W. K.; Ledgerwood, E. C.; Smith, R. A.; Murphy, M. P. Selective targeting of a redox-active ubiquinone to mitochondria within cells. Antioxidant and antiapoptotic properties. *J. Biol. Chem.* **276:**4588–4596; 2001.

[18] Koren, R.; Hadari-Naor, I.; Zuck, E.; Rotem, C.; Liberman, U. A.; Ravid, A. Vitamin D is a pro-oxidant in breast cancer cells. *Cancer Res.* **61:**1439–1444; 2001.

[19] Sato, N.; Iwata, S.; Nakamura, K.; Hori, T.; Mori, K.; Yodoi, J. Thiol-mediated redox regulation of apoptosis. Possible roles of cellular thiols other than glutathione in T cell apoptosis. *J. Immunol.* **154:**3194–3203; 1995.

[20] Singh, I.; Pahan, K.; Khan, M.; Singh, A. K. Cytokine-mediated induction of ceramide production is redox-sensitive. Implications to proinflammatory cytokine-mediated apoptosis in demyelinating diseases. *J. Biol. Chem.* **273:**20354–20362; 1998.

[21] Cai, J.; Jones, D. P. Superoxide in apoptosis, mitochondrial generation triggered by cytochrome *c* loss. *J. Biol. Chem.* **273:** 11401–11404; 1998.

[22] Elbim, C.; Pillet, S.; Prevost, M. H.; Preira, A.; Girard, P. M.; Rogine, N.; Matusani, H.; Hakim, J.; Israel, N.; Gougerot-Pocidalo, M. A. Redox and activation status of monocytes from human immunodeficiency virus-infected patients: relationship with viral load. *J. Virol.* **73:**4561–4566; 1999.

[23] Garcia-Ruiz, C.; Colell, A.; Mari, M.; Morales, A.; Fernandez-Checa, J. C. Direct effect of ceramide on the mitochondrial electron transport chain leads to generation of reactive oxygen species. Role of mitochondrial glutathione. *J. Biol. Chem.* **272:** 11369–11377; 1997.

[24] Gottlieb, E.; Vander Heiden, M. G.; Thompson, C. B. Bcl-x(L) prevents the initial decrease in mitochondrial membrane potential and subsequent reactive oxygen species production during tumor necrosis factor $\alpha$-induced apoptosis. *Mol. Cell. Biol.* **20:**5680–5689; 2000.

[25] Kirkland, R. A.; Franklin, J. L. Evidence for redox regulation of cytochrome *c* release during programmed neuronal death: antioxidant effects of protein synthesis and caspase inhibition. *J. Neurosci.* **21:**1949–1963; 2001.

[26] Satoh, T.; Sakai, N.; Enokido, Y.; Uchiyama, Y.; Hatanaka, H. Survival factor-insensitive generation of reactive oxygen species induced by serum deprivation in neuronal cells. *Brain Res.* **733:** 9–14; 1996.

[27] Shaulian, E.; Schreiber, M.; Piu, F.; Beeche, M.; Wagner, E. F.; Karin, M. The mammalian UV response: c-Jun induction is required for exit from p53-imposed growth arrest. *Cell* **103:**897–907; 2000.

[28] Ruckdeschel, K.; Mannel, O.; Richter, K.; Jacobi, C. A.; Trulzsch, K.; Rouot, B.; Heesemann, J. Yersinia outer protein P of Yersinia enterocolitica simultaneously blocks the nuclear factor-$\kappa$B pathway and exploits lipopolysaccharide signaling to trigger apoptosis in macrophages. *J. Immunol.* **166:**1823–1831; 2001.

[29] Ye, J.; Wang, S.; Leonard, S. S.; Sun, Y.; Butterworth, L.; Antonini, J.; Ding, M.; Rojanasakul, Y.; Vallyathan, V.; Castranova, V.; Shi, X. Role of reactive oxygen species and p53 in chromium(VI)-induced apoptosis. *J. Biol. Chem.* **274:**34974–34980; 1999.

[30] Green, D. R; Reed, J. C. Mitochondria and apoptosis. *Science* **281:**1309–1312; 1998.

[31] Kroemer, G.; Dallaporta, B.; Resche-Rigon, M. The mitochondrial death/life regulator in apoptosis and necrosis. *Annu. Rev. Physiol.* **60:**619–642; 1998.

[32] Martinou, J. C. Apoptosis. Key to the mitochondrial gate. *Nature* **399:**411–412; 1999.

[33] Tan, S.; Sagara, Y.; Liu, Y.; Maher, P.; Schubert, D. The regulation of reactive oxygen species production during programmed cell death. *J. Cell. Biol.* **141:**1423–1432; 1998.

[34] Wong, G. H.; Elwell, J. H.; Oberley, L. W.; Goeddel, D. V. Manganous superoxide dismutase is essential for cellular resistance to cytotoxicity of tumor necrosis factor. *Cell* **58:**923–931; 1989.

[35] Mantymaa, P.; Siitonen, T.; Guttorm, T.; Saily, M.; Kinnula, V.; Savolainen, E. R.; Koistinen, P. Induction of mitochondrial manganese superoxide dismutase confers resistance to apoptosis in acute myeloblastic leukaemia cells exposed to etoposide. *Br. J. Haematol.* **108:**574–581; 2000.

[36] Keller, J. N.; Kindy, M. S.; Holtsberg, F. W.; St. Clair, D. K.; Yen, H. C.; Germeyer, A.; Steiner, S. M.; Bruce-Keller, A. J.; Hutchins, J. B.; Mattson, M. P. Mitochondrial manganese superoxide dismutase prevents neural apoptosis and reduces ischemic brain injury: suppression of peroxynitrite production, lipid peroxidation, and mitochondrial dysfunction. *J. Neurosci.* **18:**687–697; 1998.

[37] Kiningham, K. K.; Oberley, T. D.; Lin, S.; Mattingly, C. A.; St. Clair, D. K. Overexpression of manganese superoxide dismutase protects against mitochondrial-initiated poly(ADP-ribose) polymerase-mediated cell death. *FASEB J.* **13:**1601–1610; 1999.

[38] Cross, A. R.; Jones, O. T. The effect of the inhibitor diphenyleneiodonium on the superoxide generating system of neutrophils. Specific labelling of a component polypeptide of the oxidase. *Biochem. J.* **237:**111–116; 1986.

[39] Stuehr, D. J.; Fasehun, O. A.; Kwon, N. S.; Gross, S. S.; Gonzalez, J. A.; Levi, R.; Nathan, C. F. Inhibition of macrophage and endothelial cell nitric oxide synthase by diphenyleneiodonium and its analogs. *FASEB J.* **5:**98–103; 1991.

[40] Sanders, S. A.; Eisenthal, R.; Harrison, R. NADH oxidase activity of human xanthine oxidoreductase—generation of superoxide anion. *Eur. J. Biochem.* **245:**541–548; 1997.

[41] Tew, D. G. Inhibition of cytochrome P450 reductase by the diphenyliodonium cation. Kinetic analysis and covalent modifications. *Biochemistry* **32:**10209–10215; 1993.

[42] Luetjens, C. M.; Bui, N. T.; Sengpiel, B.; Munstermann, G.; Poppe, M.; Krohn, A. J.; Bauerbach, I. E.; Krieglstein, J.; Prehn, J. H. Delayed mitochondrial dysfunction in excitotoxic neuron death: cytochrome *c* release and a secondary increase in superoxide production. *J. Neurosci.* **20:**5715–5723; 2000.

[43] Majander, A.; Finel, M.; Wikstrom, M. Diphenyleneiodonium inhibits reduction of iron-sulfur clusters in the mitochondrial NADH-ubiquinone oxidoreductase (complex I). *J. Biol. Chem.* **269:**21037–21042; 1994.

[44] Brar, S. S.; Kennedy, T. P.; Whorton, A. R.; Murphy, T. M.; Chitano, P.; Hoidal, J. R. Requirement for reactive oxygen species in serum-induced and platelet-derived growth factor-induced growth of airway smooth muscle. *J. Biol. Chem.* **274:**20017–20026; 1999.

[45] Lee, Y. S.; Kang, Y. S.; Lee, S. H.; Kim, J. A. Role of NAD(P)H oxidase in the tamoxifen-induced generation of reactive oxygen species and apoptosis in HepG2 human hepatoblastoma cells. *Cell. Death Differ.* **7:**925–932; 2000.

[46] Simizu, S.; Takada, M.; Umezawa, K.; Imoto, M. Requirement of caspase-3(-like) protease-mediated hydrogen peroxide production for apoptosis induced by various anticancer drugs. *J. Biol. Chem.* **273:**26900–26907; 1998.

[47] Hayes, D. J.; Byrne, E.; Shoubridge, E. A.; Morgan-Hughes, J. A.; Clark, J. B. Experimentally induced defects of mitochondrial metabolism in rat skeletal muscle. Biological effects of the

NADH: coenzyme Q reductase inhibitor diphenyleneiodonium.. *Biochem. J.* **229:**109–117; 1985.
[48] Gomez-Diaz, C.; Villalba, J. M.; Perez-Vicente, R.; Crane, F. L.; Navas, P. Ascorbate stabilization is stimulated in $\rho^0$ HL-60 cells by CoQ10 increase at the plasma membrane. *Biochem. Biophys. Res. Commun.* **234:**79–81; 1997.
[49] Melendez, J. A.; Davies, K. J. Manganese superoxide dismutase modulates interleukin-1$\alpha$ levels in HT-1080 fibrosarcoma cells. *J. Biol. Chem.* **271:**18898–18903; 1996.
[50] Carter, W. O.; Narayanan, P. K.; Robinson, J. P. Intracellular hydrogen peroxide and superoxide anion detection in endothelial cells. *J. Leukoc. Biol.* **55:**253–258; 1994.
[51] Lash, L. H.; Sall, J. M. Mitochondrial isolation from liver and kidney: strategy, techniques, and criteria for purity. In: Lash, L. H.; Jones, D. P., eds. *Mitochondrial dysfunction*. San Diego: Academic Press; 1993:8–28.
[52] Herrmann, M.; Lorenz, H. M.; Voll, R.; Grunke, M.; Woith, W.; Kalden, J. R. A rapid and simple method for the isolation of apoptotic DNA fragments. *Nucleic Acids Res.* **22:**5506–5507; 1994.
[53] Murakami, K.; Kondo, T.; Kawase, M.; Li, Y.; Sato, S.; Chen, S. F.; Chan, P. H. Mitochondrial susceptibility to oxidative stress exacerbates cerebral infarction that follows permanent focal cerebral ischemia in mutant mice with manganese superoxide dismutase deficiency. *J. Neurosci.* **18:**205–213; 1998.
[54] Bindokas, V. P.; Jordan, J.; Lee, C. C.; Miller, R. J. Superoxide production in rat hippocampal neurons: selective imaging with hydroethidine. *J. Neurosci.* **16:**1324–1336; 1996.
[55] Macho, A.; Castedo, M.; Marchetti, P.; Aguilar, J. J.; Decaudin, D.; Zamzami, N.; Girard, P. M.; Uriel, J.; Kroemer, G. Mitochondrial dysfunctions in circulating T lymphocytes from human immunodeficiency virus-1 carriers. *Blood* **86:**2481–2487; 1995.
[56] Rothe, G.; Valet, G. Flow cytometric analysis of respiratory burst activity in phagocytes with hydroethidine and 2',7'-dichlorofluorescin. *J. Leukoc. Biol.* **47:**440–448; 1990.
[57] Benov, L.; Sztejnberg, L.; Fridovich, I. Critical evaluation of the use of hydroethidine as a measure of superoxide anion radical. *Free Radic. Biol. Med.* **25:**826–831; 1998.
[58] Robinson, J. P.; Babcock, G., F., eds. *Phagocyte function: a guide for research and clinical evaluation*. New York: John Wiley & Sons, Inc.; 1998.
[59] Budd, S. L.; Castilho, R. F.; Nicholls, D. G. Mitochondrial membrane potential and hydroethidine-monitored superoxide generation in cultured cerebellar granule cells. *FEBS Lett.* **415:** 21–24; 1997.
[60] Goldstein, J. C.; Waterhouse, N. J.; Juin, P.; Evan, G. I.; Green, D. R. The coordinate release of cytochrome *c* during apoptosis is rapid, complete, and kinetically invariant. *Nat. Cell Biol.* **2:**156–162; 2000.
[61] Han, D.; Antunes, F.; Daneri, F.; Cadenas, E. Mitochondrial superoxide anion production and release into intermembrane space. *Methods Enzymol.* **349:**271–280; 2002.
[62] Jin, Z. G.; Melaragno, M. G.; Liao, D. F.; Yan, C.; Haendeler, J.; Suh, Y. A.; Lambeth, J. D.; Berk, B. C. Cyclophilin A is a secreted growth factor induced by oxidative stress. *Circ. Res.* **87:**789–796; 2000.
[63] Lynn, S.; Gurr, J. R.; Lai, H. T.; Jan, K. Y. NADH oxidase activation is involved in arsenite-induced oxidative DNA damage in human vascular smooth muscle cells. *Circ. Res.* **86:**514–519; 2000.
[64] Li, P.; Nijhawan, D.; Budihardjo, I.; Srinivasula, S. M.; Ahmad, M.; Alnemri, E. S.; Wang, X. Cytochrome *c* and dATP-dependent formation of Apaf-1/caspase-9 complex initiates an apoptotic protease cascade. *Cell* **91:**479–489; 1997.
[65] Enari, M.; Sakahira, H.; Yokoyama, H.; Okawa, K.; Iwamatsu, A.; Nagata, S. A caspase-activated DNase that degrades DNA during apoptosis, and its inhibitor ICAD. *Nature* **391:**43–50; 1998.
[66] Nemoto, S.; Takeda, K.; Yu, Z. X.; Ferrans, V. J.; Finkel, T. Role for mitochondrial oxidants as regulators of cellular metabolism. *Mol. Cell. Biol.* **20:**7311–7318; 2000.

## ABBREVIATIONS

DPI—diphenyleneiodonium
EB—ethidium bromide
FCS—fetal calf serum
HBSS—Hank's balanced salt solution
HE—hydroethidium
IDP—diphenyliodonium
JC-1—5,5',6,6'-tetrachloro-1,1',3,3'-tetraethylbenzimidazolylcarbocyanine iodide
MMP—mitochondrial membrane potential
MnSOD—magnesium superoxide dismutase
PBS—phosphate-buffered saline
PI—propidium iodide
PMSF—phenylmethylsulfonyl fluoride
PVDF—polyvinylidene difluoride
ROS—reactive oxygen species
Tiron—4,5-dihydroxy-1,3-benzene-disulfonic acid